scientific reports

Check for updates

EN

Network-nodal tACS induces right-lateralization of thalamocortical connectivity

Seulgi Lee[1,2,3,11], Bumhee Park[1,2,4,5,6,11], Jeehye Seo[7] & Byoung-Kyong Min[7,8,9,10]✉

Almost all functional processing in the cortex heavily relies on thalamic interactions. Since neural interactions across thalamocortical networks are essential for regulating cognitive functions, we investigated whether network-level transcranial alternating current stimulation (tACS) could modulate the functional connectivity of thalamocortical networks. Using network-node-based tACS and functional MRI (fMRI) data from the color flickering task, we performed functional connectivity and modularity analyses. Notably, tACS applied to key nodes of canonical functional networks resulted in right-lateralized thalamocortical connectivity. Compared to tACS applied to the medial prefrontal cortex (mPFC), tACS applied to the dorsolateral prefrontal cortex (dlPFC) significantly enhanced functional connectivity within the control and attentional networks. Further analyses of modularity and hub scores revealed functional clustering among sensory-visual, associative, and executive-control thalamocortical modules, along with a significant enhancement in thalamocortical interplay within the cluster. TACS-to-dlPFC enhanced interactions within the visual network, whereas tACS-to-mPFC enhanced interactions within the control network. Taken together, this study demonstrates the feasibility of network-based tACS for modulating task-relevant brain functional organization, with potential applications in cognitive impairment and clinical populations.

Keywords Conscious perception, Mental representation, Functional magnetic resonance imaging, Non-invasive electrical brain stimulation, Transcranial alternating current stimulation, Thalamocortical network, Graph network, Modularity

The experience of conscious perception of mental representations is a fundamental aspect of human cognition; however, the neural mechanisms supporting this process remain underexplored. Recent debates on the neural mechanisms underlying conscious perception have increasingly highlighted the significance of thalamocortical networks[1–3]. The thalamus is commonly regarded as the central hub—or gateway—for transmitting nearly all sensory information (excluding olfactory input) to specific cortical regions via direct thalamocortical pathways[4,5]. As such, dynamic interactions between the thalamus and the cortex are considered vital for fundamental perceptual and cognitive operations.

Building on this understanding, the present study employed a color flickering task to examine whether thalamic gating mechanisms are fundamental to the conscious experience of mental representations. Specifically, we explored whether thalamocortical interactions are essential for perceiving an illusory color generated from alternating physical stimuli. Because this form of perception occurs without a direct physical substrate, it offers a unique opportunity to investigate the neural mechanisms of conscious perception. In our task, participants viewed rapidly alternating red and green stimuli. Occasionally, this rapid flicker evoked the perceptual fusion of the two colors into a new, illusory orange. Notably, the same physical stimulus could yield either fused (orange) or non-fused percepts across trials within the same individual, allowing us to isolate the neural

[1]Department of Biomedical Informatics, Ajou University School of Medicine, Suwon 16499, Korea. [2]Department of Biomedical Sciences, Graduate School of Ajou University, Suwon 16499, Korea. [3]Department of Intelligent Precision Healthcare Convergence, Sungkyunkwan University, Suwon 16419, Korea. [4]Office of Biostatistics, Medical Research Collaborating Center, Ajou Research Institute for Innovative Medicine, Ajou University Medical Center, Suwon 16499, Korea. [5]Department of Convergence Healthcare Medicine, Graduate School of Ajou University, Suwon 16499, Korea. [6]BK21 R&E Initiative for Advanced Precision Medicine, Suwon 16499, Korea. [7]Learning Sciences Research Institute, College of Education, Seoul National University, Seoul 08826, Korea. [8]Transdisciplinary Learning Sciences, College of Education, Seoul National University, Seoul 08826, Korea. [9]Interdisciplinary Program in Neuroscience, College of Natural Sciences, Seoul National University, Seoul 08826, Korea. [10]Interdisciplinary Program in Cognitive Science, College of Humanities, Seoul National University, Seoul 08826, Korea. [11]These authors contributed equally: Seulgi Lee and Bumhee Park. ✉email: min.bk@snu.ac.kr

correlates of conscious perception under identical sensory conditions. In previous research, we conducted a color flickering experiment to investigate thalamocortical interactions associated with conscious perception using magnetoencephalography (MEG)[6] and functional magnetic resonance imaging (fMRI)[7]. By comparing physically present individual red/green colors with their illusory fused orange counterpart, thalamocortical inhibitory coupling between the thalamus and visual cortex was identified as a critical mechanism underlying conscious perception.

Furthermore, by applying transcranial alternating current stimulation (tACS) to the medial prefrontal region (a key node of the default-mode network), we observed suppressed hemodynamic activation in higher-order subthalamic and central executive networks associated with the perception of fused colors[8]. This finding suggests that higher-order thalamocortical and default-mode networks play a crucial role in humans' conscious perception of mental representations. These findings provided both theoretical[9] and empirical[6,7] evidence supporting the pivotal role of the thalamocortical inhibitory network in conscious mental representation.

Building on this, the current study aims to explore the functional connectivity within task-relevant thalamocortical and higher-order networks while applying tACS to representative nodes of mutually antagonistic networks (the dorsolateral prefrontal cortex [dlPFC] for the central executive network [CEN] and the medial prefrontal cortex [mPFC] for the default-mode network [DMN]). TACS to the primary visual cortex (V1) served as a control for the lower hierarchy of the visual processing stage. This investigation was conducted while participants performed the color flickering task. The conscious experience of mental representations is thought to require repeated and integrated interactions between specific thalamic subdivisions and their associated cortical areas[9]. This awareness is progressively enhanced as higher-order relay signals are transmitted through relevant thalamocortical circuits in a cumulative manner. Functional connectivity analysis offers a dynamic perspective on the neurophysiological interactions between thalamic relay nuclei and corresponding cortical regions, further elucidating their roles in the conscious perception process. Prior literature has established the involvement of first-order and higher-order thalamic relay nuclei—such as the lateral geniculate nucleus (LGN) and pulvinar—in visual processing, emphasizing their cumulative contributions to refined conscious perception[10]. Moreover, the interplay between the CEN, DMN, and the salience network (SN) regulates neural dynamics underlying cognitive functions[11–14]. Compared to typical nodal-based tACS, network-level tACS—particularly when alternately administered to either the CEN or DMN, leveraging their anti-correlated relationship during cognitive performance (Fig. 1)—has gained increasing attention due to its refined and potent

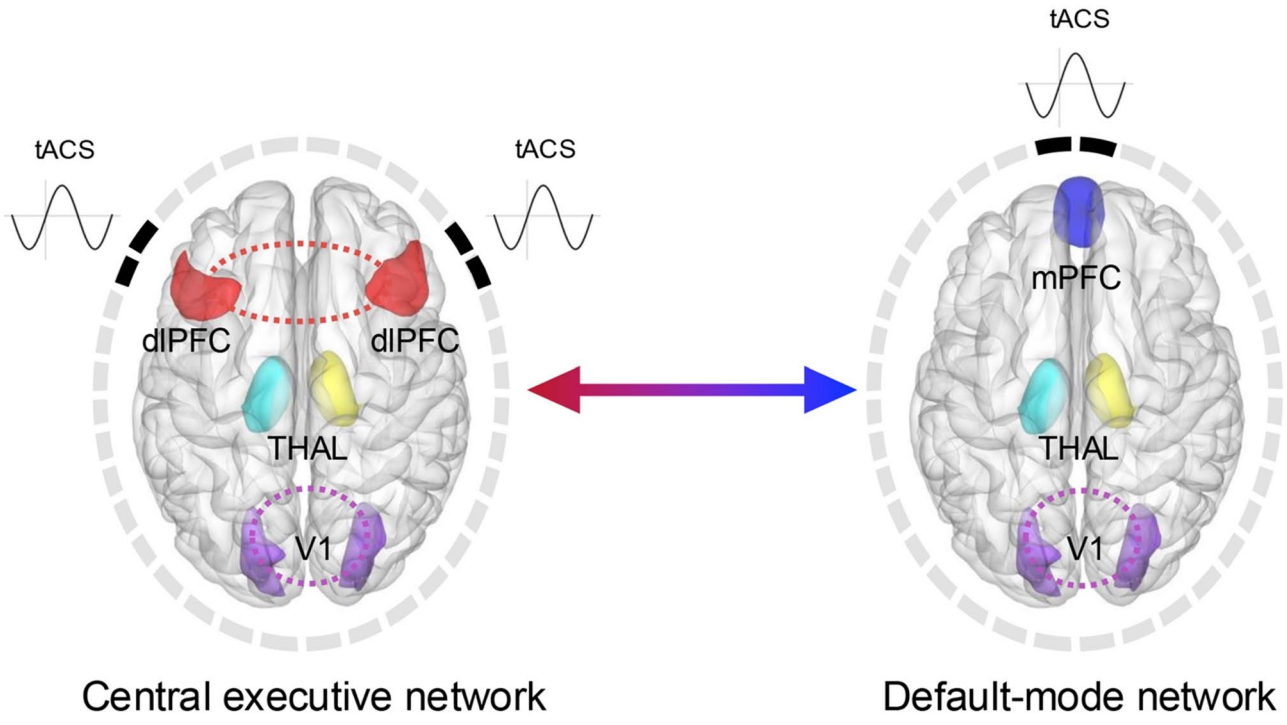

Fig. 1. Network-level tACS model. tACS leverages the anti-correlated relationship between the central executive network (CEN, shown in red) and the default-mode network (DMN, shown in blue). Network-level tACS was applied using a multi-electrode setup designed to alternately modulate the CEN and DMN. The representative nodes of the CEN (i.e., dlPFC) and the DMN (i.e., mPFC) were targeted for network-nodal tACS administration. Additionally, tACS applied to the primary visual cortex (V1, shown in purple) served as a control for the lower hierarchy of the visual processing stage. To consider lateralized thalamocortical networks during tACS, the left thalamus (shown in cyan) and the right thalamus (shown in yellow) are individually highlighted. Abbreviations: *dlPFC* dorsolateral prefrontal cortex, *mPFC* medial prefrontal cortex, *V1* primary visual cortex, *THAL* thalamus.

neuromodulatory effects reported in recent studies[8,15–17]. The anti-correlated relationship between the CEN and DMN during most cognitive functions has been well established[12,18]. For instance, during most cognitive functions, cognitive states that activate the CEN typically deactivate the DMN, and vice versa[19–21]. Thus, we examined whether network-nodal tACS significantly modulates functional connections across thalamocortical networks during the conscious perception of mental representations.

In this study, we applied functional connectivity analysis to investigate network interactions during the conscious perception of mental representations using network-level tACS (alternately targeting the CEN and DMN) in a previously validated color flickering task paradigm[6–8]. To achieve this, we analyzed thalamocortical functional connectivity across 200 cortical regions[22] and 14 thalamic regions[23] for each hemisphere. During the color flickering task, participants were presented with rapidly alternating red and green stimuli, which occasionally induced the illusory perception of a fused orange color. This paradigm allowed us to compare distinct conscious perceptions of mental representation (fusion vs. non-fusion) elicited under identical physical conditions, effectively isolating top-down subjective experience from bottom-up sensory inputs.

By investigating functional connectivity patterns across these regions, this study aims to examine the interaction between two key brain networks—namely, the CEN and DMN—which are critically involved in the high-order conscious perception of mental representations during a color flickering task. Our findings will expand the understanding of network-level interactions in conscious perception, complementing prior structural and neuromodulatory evidence[6–8]. This approach underscores the importance of thalamocortical and large-scale network dynamics in shaping subjective cognitive experiences.

Results

Since the identical physical presentation of the 50-ms flickering stimulus occasionally elicited distinct perceptual responses (fusion vs. non-fusion), the present tACS–fMRI study specifically employed the 50-ms flickering condition. During the entire fMRI scanning session of the color-flickering task, tACS was delivered online. Participants took part in two experimental sessions, during which they received two randomly assigned treatments among no-tACS, tACS-to-V1, tACS-to-mPFC, and tACS-to-dlPFC. Targeted regions for tACS included the left/right V1, mPFC (a primary DMN node), and left/right dlPFC (a primary CEN node). In the 'no-tACS' condition, participants performed the color flickering task without tACS. The color flickering task was repeated in each run to assess the impact of tACS on color perception performance.

Behavioral data

A significant interaction effect was found between response types and tACS conditions ($F(3, 60) = 7.3482$, $p = 0.0003$, partial $\eta^2 = 0.269$). Post-hoc tests revealed that all tACS conditions resulted in significantly more fusion perceptual responses than non-fusion perceptual responses (tACS-to-V1: $p = 0.0050$; tACS-to-dlPFC: $p = 0.0091$; tACS-to-mPFC: $p < 0.0001$). Additionally, in fusion perception compared to non-fusion perception, the tACS-to-V1 ($p = 0.0011$) and tACS-to-mPFC ($p = 0.0002$) conditions produced significantly more responses than the no-tACS condition.

tACS effect on brain functional connectivity

We observed no significant hemispheric difference in baseline thalamocortical functional connectivity strength in the no-tACS condition. In contrast to the absence of significant tACS-mediated differences in functional connectivity in the non-fusion condition, the fusion condition showed significant tACS-dependent changes. Notably, while no significant effects of tACS on functional connectivity were observed across the cortex and the left thalamus, tACS resulted in significant functional connectivity between 10 cortical regions and the right thalamus after false discovery rate (FDR) correction (Figs. 2 and 3A, and Table S1). The cortical areas corresponding to these tACS-affected functional connections were distributed across the salience/ventral attention, control, visual, dorsal attention, and auditory networks. Since the main effects of tACS were observed in these 10 thalamocortical regions, post hoc tests were conducted to identify the specific tACS condition responsible for significant changes in functional connectivity. As shown in Fig. 2 and Table S1, seven functional connections exhibited significantly greater strength with tACS applied to the dlPFC compared to the mPFC. These cortical regions were part of the visual, auditory, control, and salience/ventral attention networks.

We conducted a formal hemisphere × stimulation interaction analysis and found no significant interaction, suggesting that the effect of tACS does not differ across hemispheres. Accordingly, the observed main effect of tACS on right lateralization is unlikely to reflect hemisphere-specific modulation. In addition, we compared the simulated electric fields (E-fields) for stimulation applied to the left and right hemispheres across both stimulation targets (i.e., tACS to the dlPFC and V1). As shown in Fig. 4, no significant differences were observed between hemispheres (tACS-to-dlPFC: $t(20) = -0.498$, *n.s.*; tACS-to-V1: $t(20) = 0.789$, *n.s.*). Therefore, the right lateralization observed in the present study is unlikely to be attributable to differences in the physical properties of the stimulation.

Brain functional organization

Modularity

The no-tACS, tACS-to-V1, tACS-to-mPFC, and tACS-to-dlPFC conditions yielded modularity quality (Q) values of 0.6234, 0.5791, 0.5326, and 0.5202, respectively. As the Q values are relatively high, each module included the specific thalamocortical subregions. Since we observed consistent thalamocortical regions for each module regardless of tACS conditions, we labeled the three modules as the 'sensory-visual thalamocortical module,' 'associative thalamocortical module,' and 'executive-control thalamocortical module,' primarily based on the temporal and functional roles of each thalamocortical processing stage. Subsequently, corresponding thalamic and cortical regions were classified into each module (Fig. 5 and Table S2). The sensory-visual thalamocortical

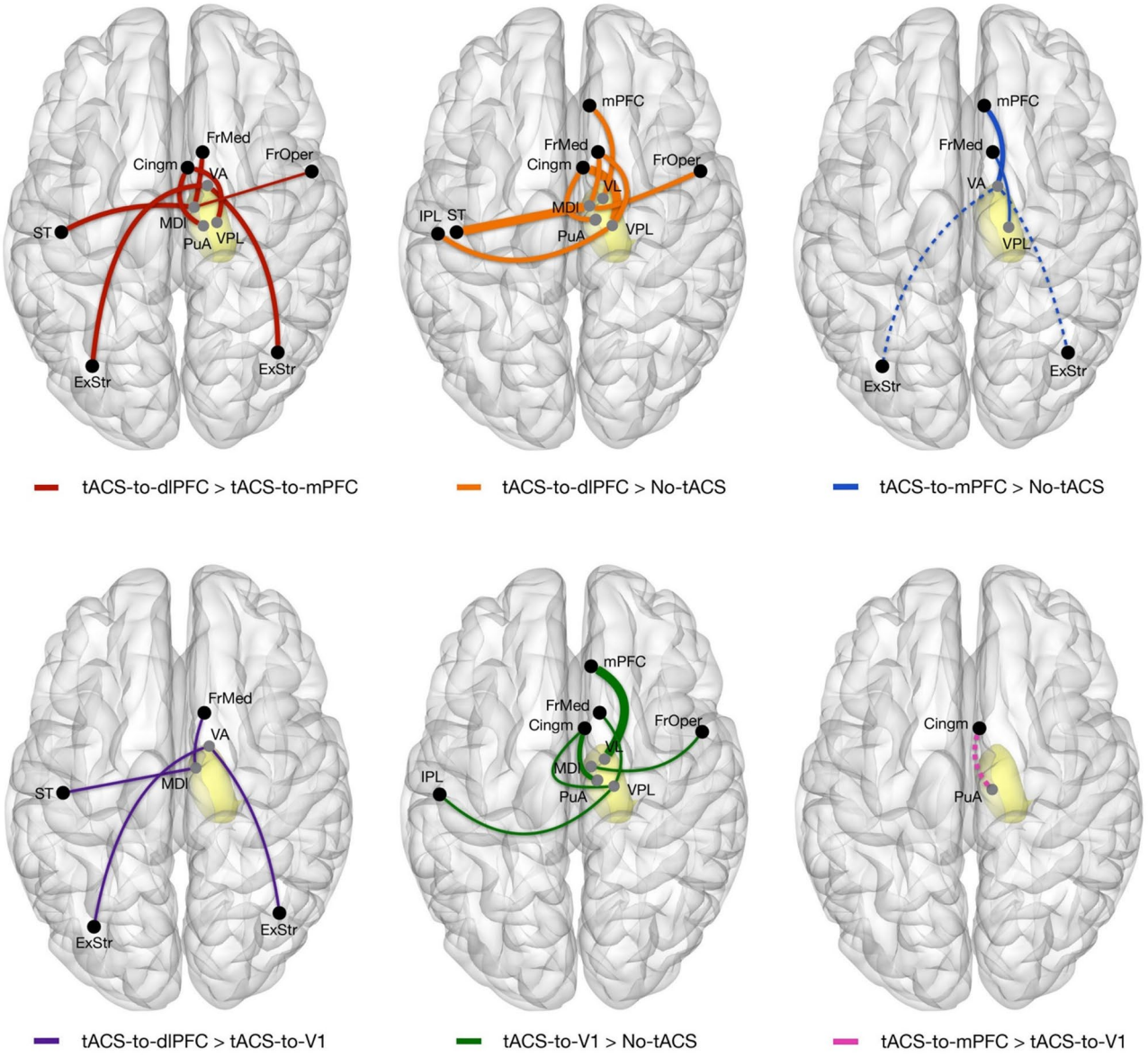

Fig. 2. Significant thalamocortical functional connectivity across tACS conditions. Red lines in the upper-left panel indicate tACS-to-dlPFC > tACS-to-mPFC, whereas purple lines in the lower-left panel indicate tACS-to-dlPFC > tACS-to-V1. Orange lines in the upper-middle panel indicate tACS-to-dlPFC > no-tACS, whereas green lines in the lower-middle panel indicate tACS-to-V1 > no-tACS. Blue lines in the upper-right panel indicate tACS-to-mPFC > no-tACS, whereas pink lines in the lower-right panel indicate tACS-to-mPFC > tACS-to-V1. Gray dots represent thalamic nodes, while black dots represent cortical nodes. Notably, all significant functional connections are linked with the right thalamus (yellow), with no significant connectivity observed in the left thalamus. Solid lines indicate stronger connectivity in the first tACS condition, whereas dotted lines indicate stronger connectivity in the second condition. Only functionally significant connections ($p < 0.05$) are shown, with line thickness reflecting connectivity strength. Abbreviations: *Cingm* mid-cingulate cortex, *dlPFC* dorsolateral prefrontal cortex, *FrMed* frontal medial cortex, *FrOper* frontal operculum, *ExStr* extrastriate cortex, *MDl* mediodorsal lateral parvocellular thalamus, *IPL* inferior parietal lobule, *mPFC* medial prefrontal cortex, *PuA* anterior pulvinar, *ST* superior temporal cortex, *VA* ventral anterior thalamus, *VL* ventral lateral thalamus, *VPL* ventral posterolateral thalamus, *V1* primary visual cortex.

module consisted of visual cortical regions and two thalamic regions [i.e., LGN and inferior pulvinar]. The associative thalamocortical module included three thalamic regions (i.e., anterior pulvinar, ventral posterolateral, and intralaminar thalamus) and 48 cortical areas associated with the somatomotor, dorsal attention, salience/ventral attention, and auditory networks. The executive-control thalamocortical module comprised six thalamic subdivisions (i.e., anteroventral nucleus, lateral posterior, ventral anterior, ventral lateral, mediodorsal medial magnocellular, and mediodorsal lateral parvocellular thalamus) and 50 cortical regions linked to the control, default, salience/ventral attention, language, and dorsal attention-related networks. Notably, this categorization

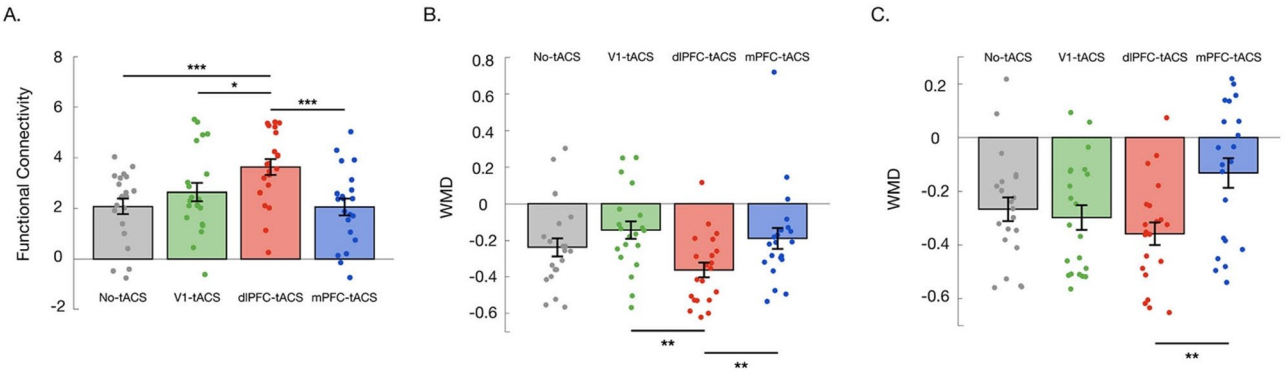

Fig. 3. tACS region-dependent functional connectivity and WMD scores. The left panel (**A**) shows functional connectivity values (*z*-scores) between the right mediodorsal lateral parvocellular thalamus (MDl.R) and the right medial frontal cortex (FrMed2.SAA.R) across different tACS conditions: no-tACS (gray), tACS-to-V1 (green), tACS-to-dlPFC (red), and tACS-to-mPFC (blue). The middle panel (**B**) presents WMD scores within the right lateral prefrontal cortex (PFCl1.ContC.R) across different tACS conditions. The right panel (**C**) displays WMD scores within the left medial posterior prefrontal cortex (PFCmp1.ContB.L) across different tACS conditions. Asterisks indicate statistical significance ($^{*}p < 0.05$; $^{**}p < 0.01$; $^{***}p < 0.001$). Small circles represent individual data points ($N = 21$). Error bars represent standard errors of the mean. Abbreviation: *L* left, *R* right, *ContB* control network B, *ContC* control network C, *SAA* salience/ventral attention network A, *PFCl1* lateral prefrontal cortex 1, *PFCmp1* medial posterior prefrontal cortex 1, *FrMed2* frontal medial cortex 2, *MDl* mediodorsal lateral parvocellular thalamus, *mPFC* medial prefrontal cortex, *dlPFC* dorsolateral prefrontal cortex.

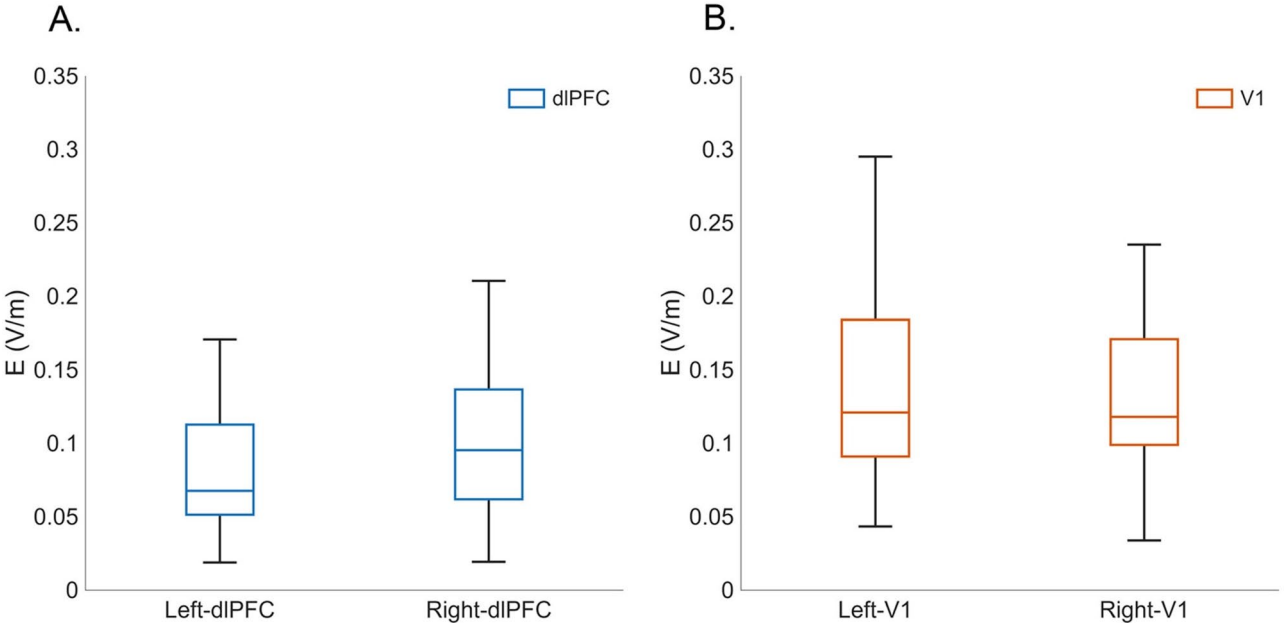

Fig. 4. Comparison of tACS-induced electric fields across the left and right hemispheres. Simulated electric field strength (V/m) during bilateral tACS applied to (**A**) the dlPFC (blue boxes) and (**B**) V1 (red boxes). For both the tACS-to-dlPFC and tACS-to-V1 conditions, no significant hemispheric differences were observed. Box plots indicate the interquartile range (first to third quartiles), with the horizontal line representing the median; whiskers extend to the minimum and maximum values. Abbreviations: *dlPFC* dorsolateral prefrontal cortex, *V1* primary visual cortex.

aligns with recent studies demonstrating a temporal sequence of thalamic activity[24,25]. Specifically, the sensory-visual thalamocortical module reflects the role of thalamic subregions in mediating inter-regional coupling and top-down communication across large-scale cortical networks[26–28]. The associative thalamocortical module corresponds to nuclei such as the intralaminar (centromedian) nucleus, which exhibits the earliest activation during behavioral arousal transitions[29,30]. It has also been consistently reported that the ventral posterolateral

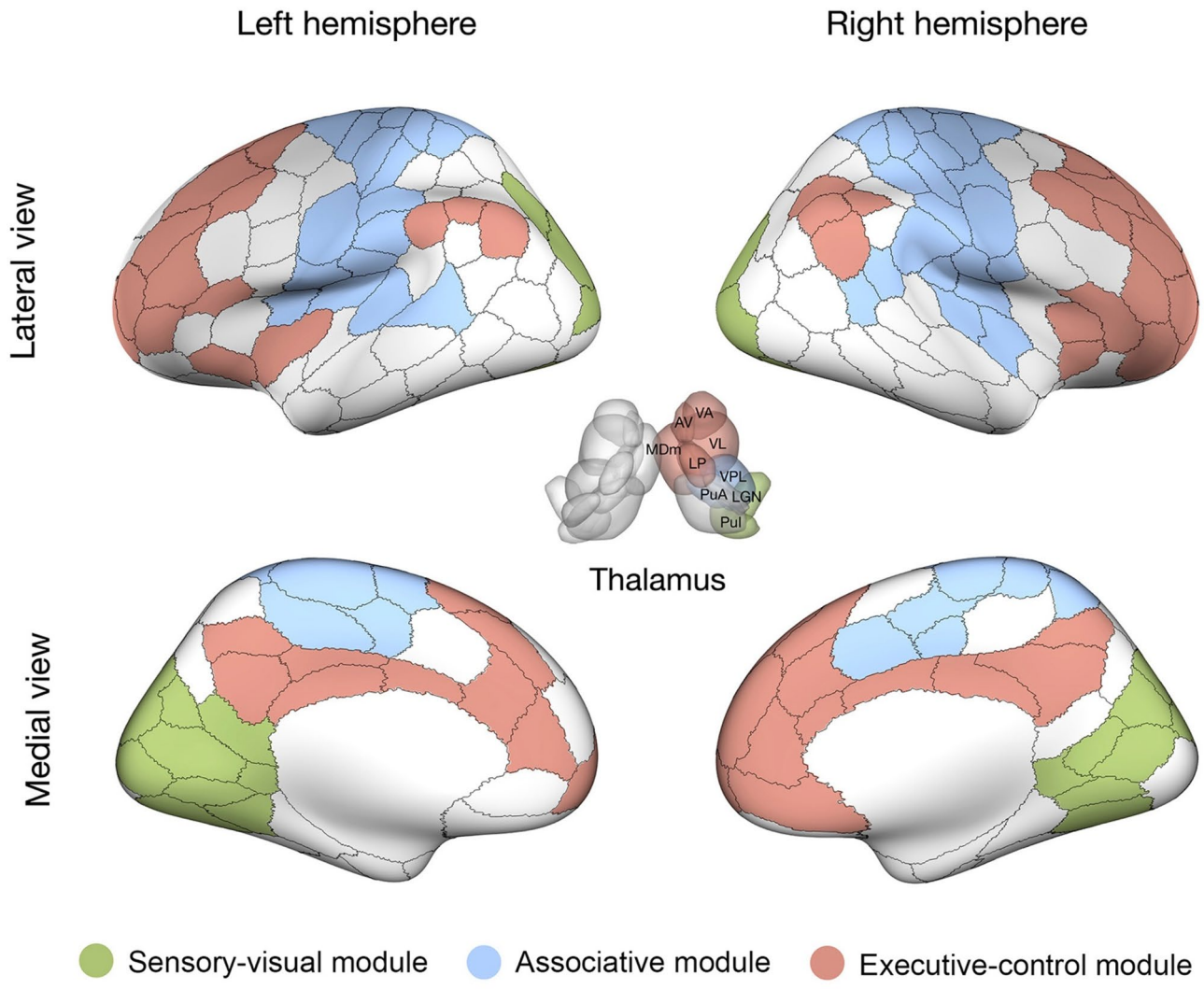

Fig. 5. Three thalamocortical modules. Modularity analysis identified three distinct functional clusters: the sensory-visual thalamocortical module (green), the associative thalamocortical module (blue), and the executive-control thalamocortical module (red). The left panel represents the left hemisphere, while the right panel represents the right hemisphere. The upper sections represent the lateral view, while the lower sections represent the medial view. The inset highlights thalamic subdivisions. The thalamus is shown from a dorsal view, with the top oriented toward the anterior side. Notably, only the right thalamus exhibited significant thalamocortical functional connections. Modules were estimated accordingly, with the included right thalamic regions highlighted in color. These thalamocortical modules remained consistent across different tACS conditions. A detailed list of thalamic and cortical regions for each module is provided in Table S2. Abbreviations: *AV* anteroventral nucleus, *LGN* lateral geniculate nucleus, *LP* lateral posterior, *MDm* mediodorsal medial magnocellular, *PuA* pulvinar anterior, *PuI* pulvinar inferior, *VA* ventral anterior, *VL* ventral lateral, *VPL* ventral posterolateral.

thalamic nucleus activates earlier[24]. Finally, the executive-control thalamocortical module aligns with higher-order nuclei, including the mediodorsal thalamus, which are known to support sustained delay-period activity and prolonged modulation of cortical processing[31–33]. Together, these categorizations highlight how distinct thalamocortical components contribute sequentially and interactively to information processing.

Hub scores

We calculated hub scores, specifically the participation coefficient (PC) and within-module degree (WMD), to indicate the degree of interconnection between clusters and within individual clusters, respectively. Consistent with a previous study[5], hub score levels differed between thalamic and cortical regions. The mean PC scores of the right thalamic areas were 0.5493, 0.5412, 0.5067, and 0.5420 for the no-tACS, tACS-to-V1, tACS-to-mPFC, and tACS-to-dlPFC conditions, respectively, while the mean PC scores of the cortical regions were 0.3331, 0.3183, 0.3330, and 0.2956 for the same conditions. The WMD values of the right thalamic subregions were

3.2407, 3.1276, 3.1662, and 3.0579, whereas those of the cortical areas were −0.2269, −0.2189, −0.2216, and −0.2141 for the same conditions.

Statistical analysis was performed on PC and WMD scores for each cortical and thalamic region that remained consistent across modules, regardless of tACS conditions. A significant main effect of tACS, FDR-corrected, was found in WMD scores but not in PC scores (Table S3). Subsequent tests were conducted to identify the specific tACS condition responsible for significant effects on WMD scores. When comparing the effects of tACS-to-mPFC and tACS-to-dlPFC, cortical regions within the visual network (i.e., the extrastriate cortex and fusiform area) exhibited significantly greater WMD scores when tACS was applied to the dlPFC compared to the mPFC (Table S3). Conversely, in the tACS-to-mPFC condition relative to tACS-to-dlPFC, significantly higher WMD values were observed in the ventral anterior thalamus and cortical regions associated with the control network (i.e., the mPFC, dlPFC, orbitofrontal cortex, and inferior parietal lobule; Fig. 3BC and Table S3).

Discussion

The present study revealed the non-invasive neuromodulatory effects of tACS on functional connectivity during the conscious perception of mental representations in the color flickering task. These findings provide compelling evidence that tACS can serve as a potent tool for modulating not only node-based brain functions but also network-level interactions across key nodes. Notably, tACS applied to the primary nodes of canonical functional networks led to right-lateralized thalamocortical connectivity during the color flickering task. Further analyses of modularity and hub scores revealed functional clustering among sensory-visual, associative, and executive-control thalamocortical modules.

Compared to tACS applied to the mPFC, tACS applied to the dlPFC resulted in significantly enhanced functional connectivity within attentional and control-related thalamocortical networks (Fig. 2 and Table S1). For example, tACS to the dlPFC facilitated thalamocortical communication across higher-order thalamic subdivisions (e.g., anterior pulvinar, ventral anterior, mediodorsal lateral parvocellular, and ventral posterolateral thalamic nuclei) and cortical areas involved in control and salience/ventral attentional networks. Since the dlPFC is a key node of the central executive network[18,34], tACS applied to the dlPFC may promote neural interactions associated with control and attentional functioning during the color flickering task. From a thalamic perspective, the ventral anterior thalamus is associated with executive and attentional regulation[33]. The tACS-induced reinforcement of functional connectivity between the ventral anterior thalamus and extrastriate visual cortices suggests a tACS-modulated interplay between higher-order attentional processes and fundamental visual processing during the conscious perception of flickering colors. Consistently, we observed that tACS applied to the mPFC significantly enhanced WMD scores in the ventral anterior thalamus, indicating improved intercommunication within this region. Both the ventral anterior and mediodorsal lateral parvocellular (MDl) thalamic nuclei have strong connections with the prefrontal cortex[35,36]. MDl activity mediates prefrontal contributions to both perceptual performance[37] and executive control[38]. We observed that dlPFC-tACS strengthened functional connectivity between the MDl and the frontal salience/ventral attentional network. This is consistent with previous findings that the MDl serves as a key relay hub between sensory and cognitive systems[39,40], playing a significant role in attention, working memory, and sensory integration[41–43]. Additionally, since the anterior pulvinar is substantially involved in visual attentional processing[44–46], tACS may enhance thalamocortical interactions between the anterior pulvinar and the salience/ventral attentional network in the present study.

Notably, we observed tACS-induced, right-lateralized thalamocortical changes in task-relevant functional connectivity. Although tACS in the present study was applied bilaterally, its effect on functional connectivity was particularly evident in the right hemisphere. In line with our findings, during the presentation of color stimuli, the mean cerebral blood flow velocity in the right posterior cerebral artery was consistently greater than in the left, and the right visual cortex is known to be selectively sensitive to wavelengths[47]. It has also been reported that the left hemisphere tends to interact more exclusively with itself, particularly in cortical regions involved in language and fine motor coordination, whereas the right hemisphere is more involved in visuospatial, attentional, and non-verbal processing[48] and interacts in a more integrative manner with both hemispheres[49]. Thus, it is likely that tACS administration during the color flickering task facilitated thalamocortical interactions in an integrative manner to achieve a fused perception of the orange color, resulting in enhanced functional connectivity, particularly in the right hemisphere.

It is noteworthy that the three clustered modules correspond to the functional and temporal processing stages of thalamocortical communication. Specifically, considering the fundamental roles of subthalamic regions, one module appears to be associated with the early processing stage, while another is likely related to the late processing stage, particularly involving prefrontal functions. This classification is supported by the composition of the associative thalamocortical module, which includes the anterior pulvinar, ventral posterolateral, and intralaminar thalamus—key structures involved in the relatively early thalamocortical processing[24,25]. In contrast, the executive-control thalamocortical module consists of the ventral anterior, ventrolateral, and mediodorsal thalamus, which are strongly connected to prefrontal areas[35,36]. Additionally, the remaining module appears to represent the principal thalamocortical interaction during the color perception task, primarily involving the LGN and pulvinar. This suggests that the brain strategically utilizes network resources for visual processing in a functionally specialized manner.

Moreover, the tACS in the present study facilitated neural interactions not between modules (i.e., PC) but within modules (i.e., WMD). Specifically, tACS applied to the dlPFC significantly enhanced interaction within the visual network, while tACS applied to the mPFC significantly enhanced interaction within the control network and ventral anterior thalamus. Notably, tACS administered to the dlPFC facilitated intercommunication within the extrastriate cortex and fusiform gyrus. This aligns with the established role of the extrastriate cortex in processing specific features of visual object recognition[50,51] and the fusiform area's active correlation with color

perception[52,53]. Presumably, tACS-mediated modulation of the CEN relative to the DMN promoted the essential processing sequence of color features during the color flickering task.

Compared to tACS applied to the dlPFC, tACS applied to the mPFC significantly increased intercommunication within the control-related network, including the mPFC, dlPFC, orbitofrontal cortex, and inferior parietal cortex. This suggests that tACS applied to the mPFC efficiently modulated not only the mPFC (a key node of the DMN) but also the dlPFC (a key node of the CEN). This is plausible because the CEN and DMN are functionally connected; the CEN is mutually anti-correlated with the DMN, and their interaction is regulated by the salience network[12–14,18]. Thus, tACS administered to the mPFC could influence not only the DMN but also the CEN. Additionally, as the orbitofrontal cortex and mPFC are functionally linked, particularly in decision-making and inhibitory control[54–56], tACS applied to the mPFC was able to modulate WMD scores in the orbitofrontal cortex. Similarly, improved inter-networking within the inferior parietal cortex could be achieved by tACS applied to the mPFC during the color flickering task. This effect may be attributed not only to the functional connection between the mPFC and the inferior parietal cortex but also to the inferior parietal cortex's involvement in perception[57], response inhibition[58], and working memory[59]. Accordingly, tACS applied to the mPFC could facilitate functional interplay within the inferior parietal cortex.

However, the findings should be interpreted with caution considering several limitations. First, stimulation frequencies differed across target regions to induce resonance with their predominant oscillatory dynamics (occipital alpha, prefrontal beta), raising the possibility that observed effects may partly reflect frequency-specific influences rather than network-node targeting *per se*. Accordingly, for instance, V1-related inferences may need to be considered exploratory. To mitigate this concern, harmonically related frequencies were selected (9 Hz for occipital alpha; 18 Hz for prefrontal beta). Notably, comparisons between dlPFC and mPFC are less susceptible to this confound, as both regions were stimulated at the same beta frequency (18 Hz). Second, the no-tACS condition involved the absence of current delivery. Although this controls for task-related effects, it does not account for cutaneous sensations or arousal associated with stimulation, and therefore may not constitute a fully adequate sham control, particularly for behavioral outcomes. Third, although a clear and consistent relationship between tACS-induced neural modulation and behavioral changes would support a robust brain–behavior relationship, no detectable behavioral consequences of the neural effects were observed in the present study. Therefore, this constraint should be considered when interpreting the findings. Future studies should further refine experimental designs to address these limitations.

To sum up, our findings provide compelling evidence for the feasibility of network-level tACS administration in modulating task-relevant functional connectivity and intercommunication within the module. Almost all cortical functional processing heavily relies on thalamic interactions. Since neural interactions across thalamocortical networks are essential for regulating cognitive functions, tACS may serve as a potent tool for intentionally and selectively manipulating brain network dynamics, ultimately influencing human cognitive behavior. Furthermore, it holds potential for applications in treating cognitive impairments and clinical populations.

Materials and methods

Participants

The research included thirty-five healthy individuals (average age: 24.8 ± 2.9 years, SD; 20 males). All participants possessed normal or corrected-to-normal vision and successfully completed the Ishihara color test, verifying the absence of color blindness. They reported no history of neurological or psychiatric conditions, MRI contraindications, or current/past issues with alcohol or drug abuse or dependence. Additionally, none were using illicit substances. Each participant provided written informed consent and was compensated for their participation. The study complied with ethical guidelines established by the Institutional Review Board of Korea University (Approval No. KUIRB-2021-0209-08) and the Declaration of Helsinki (World Medical Association, 2013).

Materials and procedure

For this study, we conducted a new analysis of the dataset collected by Seo and Min[8]. The study presented stimuli using a 5 × 5 grid of 3-mm round, diffused red and green light-emitting diode (LED) lights (model number: 100F3W-YT-REGR-CA, Chanzon Technology). The grid, consisting of five rows and five columns of LEDs, was mounted on a black panel with a 1-cm gap between adjacent rows and columns. The red and green LEDs emitted wavelengths of 620–625 nm and 515–520 nm, respectively, targeting human retinal long-wave and middle-wave photoreceptors, which exhibit peak responses at mean absorbance wavelengths of 562.8 nm (red) and 533.8 nm (green), as noted by Bowmaker and Dartnall[60]. Monochromatic testing, based on the CIE 1931 RGB color-matching function, revealed maximal peak emissions of approximately 610 nm for red and 540 nm for green. To control for luminance effects, the intensity of both colors was adjusted to around 800 mcd. A thin plastic diffuser was placed over the LED grid to ensure uniform light dispersion.

The experimental design employed in this study aimed to investigate neural interactive changes in the thalamocortical network, as in the previous MEG[6] and fMRI[7,8] studies. This study employed a 50-ms flickering condition to investigate subjective perceptual differences between fusion and non-fusion conditions. Despite identical 50-ms flickering stimuli, participants occasionally reported perceiving different colors, such as red and green (non-fusion) or orange (fusion). We propose that this difference is optimal for exploring the top-down aspects of conscious perception. The presentation involved alternating red and green LED flickers, each lasting 50 ms, with trials lasting 5 s and intertrial intervals varying between 6 and 10 s (average 8 s). To prevent retinal afterimages, a 5-ms gap was introduced between consecutive red and green stimuli, allowing the previous color impressions to fade[61]. Participants were instructed to press a button with either their right or left thumb to indicate their perception of a fused orange color, with response hands balanced across participants. To minimize

movement artifacts, they were asked to press the button only after the conclusion of each 5-second flickering presentation.

During the entire fMRI scanning session (15 min 10 s) of the color-flickering task, tACS was delivered online using an MR-compatible M×N 65 high-definition (HD) transcranial electrical stimulator (tES) system (Soterix Medical Inc., New York, USA). TACS intensities were maintained below each participant's sensory threshold, with peak-to-peak amplitudes ranging from 0.2 to 1.5 mA, customized for each individual. Targeted regions for tACS included the left/right V1, mPFC (a primary DMN node), and left/right dlPFC (a primary CEN node). The SimNIBS software (ver. 3.2.6, DRCMR & DTU, Denmark)[62] and tES LAB stimulation software (ver. 3.0, Neurophet, Seoul, Korea) were used to ensure accurate targeting of stimulation areas prior to the main study (Fig. 6D). The mean electric field intensity reached 0.12 V/m at the stimulated cortical regions.

Participants took part in two experimental sessions, each spaced at least two days apart, during which they received two randomly assigned treatments among no-tACS, tACS-to-V1, tACS-to-mPFC, and tACS-to-dlPFC. In the 'no-tACS' condition, participants performed the color flickering task without tACS. Both participants and examiners were blinded to the type of stimulation administered. Each session comprised two fMRI scanning runs, with each run assigned a different tACS treatment and separated by a short break. The order of tACS treatments was counterbalanced among participants. The color flickering task was repeated in each run to assess the impact of tACS on color perception performance, with thirty trials per run in the 50-ms flickering condition.

To align the 50-ms flickering frequency with perceptual processing, 9 Hz was used when consecutive inputs of two colors were perceived as a single unit (100 ms with a 10-ms gap), and 18 Hz was used when each color was perceived as an individual unit (50 ms with a 5-ms gap). Both frequencies were employed as tACS stimulation frequencies. Given that electroencephalography (EEG) alpha activity predominantly occurs in the occipital region and EEG beta activity is associated with top-down processing in the prefrontal region[63–65], 9 Hz (alpha band) was applied to V1 (tACS-to-V1), while 18 Hz (beta band) was applied to the prefrontal region (targeting the dlPFC and mPFC; tACS-to-dlPFC and tACS-to-mPFC). Although the occipital alpha frequency (9 Hz) and frontal beta frequency (18 Hz) were chosen for the respective tACS conditions, these distinct frequencies might induce different brain activation patterns, which should be considered when interpreting the results. As shown in Fig. 6C, a sample channel montage illustrating the placement of both stimulation input electrodes and surrounding return electrodes[8]. The currents of all stimulation and return channels were adjusted to ensure that the total current sum remained at zero.

FMRI data acquisition

MR images were acquired using a Siemens 3T MAGNETOM Trio Tim Syngo scanner (Siemens Healthcare, Erlangen, Germany) equipped with a 32-channel head coil. Participants were briefed on the experimental procedure and familiarized with the setup and stimuli prior to the experiment. They were instructed to keep their eyes open and focus on the LED panel located outside the MRI shielding room, visible through a mirror attached to the head coil. The LED light, viewed through an electromagnetically shielded window, was positioned approximately 520 cm from the participants, creating a visual angle of 0.8°. To enhance color perception, the LED flickering experiment was conducted in a dark environment, both inside and outside the MRI shielding room.

FMRI data were acquired using an echo-planar imaging (EPI) sequence, with the initial 5 volumes (~ 10 s) discarded, yielding a total of 455 volumes (~ 15 min 10 s) [repetition time (TR) = 2,000 ms, echo time (TE) = 30 ms, flip angle (FA) = 90°, multi-band acceleration factor = 3, acquisition matrix = 96 × 96, field of view (FOV) = 192 × 192 mm^2, in-plane voxel size = 2 × 2 × 2 mm^3, 75 transverse slices, no slice gap]. After the fMRI data collection, three-dimensional anatomical images were obtained using a magnetization-prepared rapid gradient-echo (MP-RAGE) for each participant [TR = 2,300 ms, TE = 2.13 ms, inversion time (TI) = 0.9 s, FA = 9°, acquisition matrix = 256 × 256, in-plane voxel size = 1 × 1 × 1 mm^3, 224 sagittal slices].

Spatial pre-processing for fMRI data

MRI data pre-processing was performed using SPM12 (https://www.fil.ion.ucl.ac.uk/spm/software/spm12). Standard task-based fMRI pre-processing steps were applied, including slice-timing correction (with the first slice as the reference), realignment for motion correction, co-registration, segmentation of gray and white matter, normalization to the Montreal Neurological Institute (MNI) template, and spatial smoothing using a 6-mm full-width at half-maximum (FWHM) Gaussian kernel. To reduce potential head-motion effects, participants were excluded based on the following criteria: (1) average head movement (frame-wise displacement, FD) exceeding 0.2 mm and (2) more than 30% of volumes showing high motion (relative FD > 0.2 mm). As a result, five participants were excluded due to excessive motion during the fMRI session. Additionally, nine participants were excluded for the following reasons: three were unexpectedly taking psychotropic medications before the experiment, five exhibited one-directional responses (all non-fusion) during the no-tACS fMRI session, and one reported one-directional responses (all non-fusion) during the tACS-to-dlPFC session. Ultimately, behavioral and neuroimaging data from 21 participants were included in the analysis. As the typical fMRI results were reported in our previous study[8], the present study focused on network analyses.

Thalamocortical functional connectivity

Significant alterations in thalamocortical functional connectivity suggest that tACS may modulate specific information flows in the brain, with even minor fluctuations potentially influencing functional organization. To clarify the neuromodulatory mechanisms underlying tACS effects on brain network dynamics, we examined its influence on functional connectivity. The brain regions were defined using the Schaefer 200 atlas for cortical regions[22] and the Automated Anatomical Labeling 3 (AAL3) atlas for bilateral thalamic regions[23]. For each region of interest (ROI), regionally averaged fMRI time series were extracted and temporally preprocessed using

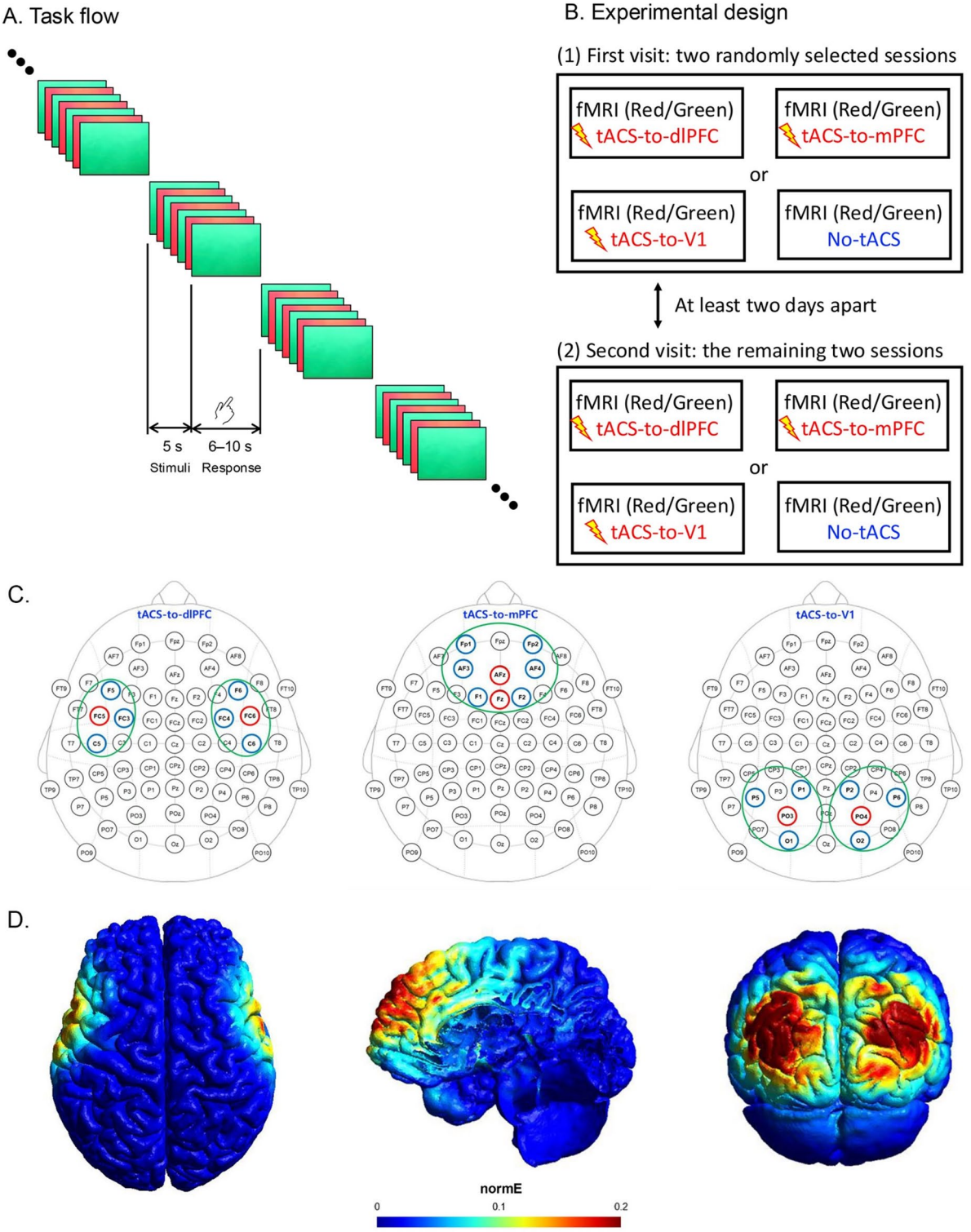

standard procedures: (1) linear detrending, (2) removal of confounding effects from six rigid motion parameters, their derivatives, and five principal components derived from white matter and cerebrospinal fluid (CSF) masks, and (3) band-pass filtering (0.009–0.25 Hz) to capture low-frequency fluctuations in fMRI signals[66–70]. Functional connectivity was estimated by calculating the Pearson correlation coefficient between the time series of each pair of regions. All correlation coefficients were normalized via Fisher's r-to-z transformation to improve normality for further analyses. These procedures were repeated for each tACS condition (no-tACS, tACS-to-V1, tACS-to-mPFC, and tACS-to-dlPFC). To examine associations between bilateral thalamic areas and cortices, statistical analyses were conducted separately for right-thalamocortical and left-thalamocortical connections (i.e., a total of 2,800 functional connections = 200 cortical areas × 14 thalamic areas).

◀**Fig. 6**. Experimental design and tACS neuromodulation. (**A**) Red and green LED stimuli alternated in 50-ms flickers within 5-s trials, with intertrial intervals of 6–10 s (mean 8 s). Participants indicated the perception of a fused orange color by pressing a button. To minimize motion artifacts, responses were made only after the end of each 5-s flickering presentation. (**B**) Participants completed two experimental sessions separated by at least two days, receiving two randomly assigned conditions from four treatments (tACS-to-dlPFC, tACS-to-mPFC, tACS-to-V1, and no-tACS). During the entire fMRI scanning session (15 min 10 s) of the color-flickering task, tACS was delivered online. In the no-tACS condition, the color-flickering task was performed without electrical stimulation. (**C**) tACS channel montage for tACS to the dlPFC (left), tACS to the mPFC (middle), and tACS to V1 (right). Red indicates the stimulation channels, while blue represents the surrounding return channels. Each green ring marks a modular subset of stimulation and return channels for each target region. The number of tACS channels was matched across the three tACS conditions. (**D**) Simulation of the tACS-induced electric field when tACS was administered to the dlPFC (left; top view), the mPFC (middle; sagittal view), and V1 (right; back view). The unit *normE* denotes the normalized strength of the induced electric field (V/m), with high intensities indicated in red and low intensities in blue. Abbreviations: *dlPFC* dorsolateral prefrontal cortex, *mPFC* medial prefrontal cortex, *V1* primary visual cortex.

Modularity and hub scores

By defining modularity and estimating hub scores of the brain for each tACS condition, we explored the neuromodulatory effects of tACS on brain functional organization. Modularity describes how the brain is organized into modules, allowing for specialization within distinct systems. In addition, hub scores represent the degree of interconnection between clusters and within each cluster. We applied this network analysis to thalamocortical functional connections across the bilateral cortex and thalamus.

The thalamocortical functional connections were clustered using modularity optimization and consensus clustering[71]. After confirming the robustness of the modularity results across thresholds (10–50%, in 5% increments), the top 30% of the functional connectivity matrix was selected as a representative threshold for modularity estimation. To construct a symmetric matrix, a zero block matrix was added, corresponding to the number of regions within the cortex ($n = 200$) and thalamus ($n = 14$), resulting in a 214×214 symmetric matrix[72]. To validate the optimized module structure, the modularity quality (Q) value was calculated for each modularity configuration[73]. All thalamocortical connections in each tACS condition were divided into three modules. Subsequently, we evaluated the Q value, which indicates how well nodes in a network are categorized into modules. The Q values typically range between 0.3 and 0.7 in networks with meaningful modular organization[74], and values above 0.3 generally indicate the presence of significant community structures within a network[75].

Furthermore, we calculated hub scores, including the participation coefficient (PC) and within-module degree (WMD), to evaluate node properties[76]. The PC reflects the extent to which a node connects across different modules, while the WMD measures the degree centrality within its own module. Nodes with relatively higher PC scores are more likely to function as connector hubs, facilitating inter-modular connectivity, compared to those with lower scores. In contrast, nodes with higher WMD scores are more likely to act as provincial hubs, primarily collaborating within their own module.

Statistical analysis

A two-way repeated measures analysis of variance (ANOVA) was conducted to assess the effects of tACS conditions (no-tACS, tACS-to-V1, tACS-to-mPFC, and tACS-to-dlPFC) and response types (fusion and non-fusion) on perceptual outcomes during the color-flickering task. The perceptual outcomes were measured by the number of button presses for each of the fusion and non-fusion perceptions. Under the no-tACS condition, we analyzed the main effect of hemisphere (FDR-corrected) to investigate hemispheric differences in baseline thalamocortical functional connectivity. Additionally, a one-way repeated measures ANOVA was performed to determine whether functional connectivity varied across tACS conditions. A one-way repeated measures ANOVA was conducted across all 2,800 connections (200 cortical × 14 thalamic). Connections exhibiting a significant main effect of tACS (FDR-corrected) were subsequently identified, followed by post hoc comparisons. After analyzing the impact of tACS on thalamocortical functional connectivity, network analyses were applied to the functional connectivity matrix.

For each tACS condition, modularity was identified as a characteristic module, and a one-way repeated measures ANOVA was used to evaluate differences in hub scores across tACS conditions. When significant main effects of tACS were detected in thalamic or cortical regions, post hoc tests were conducted to identify the specific tACS condition responsible for these effects. To address multiple comparison issues across multiple functional nodes or connections, the false discovery rate (FDR) correction was applied (FDR < 0.05). All analyses were conducted using MATLAB (ver. R2021a, MathWorks, Natick, USA), and modularity and hub scores were calculated using the Brain Connectivity Toolbox (BCT: https://sites.google.com/site/bctnet/)[77].

Data availability

Anonymized derivatives (e.g., unthresholded statistical maps) will be made available when feasible. The data and analytical tools used in this study are available from the corresponding author upon reasonable request.

Received: 31 January 2026; Accepted: 6 April 2026
Published online: 12 April 2026

References

1. Edelman, G. M. & Tononi, G. *A universe of consciousness: How matter becomes imagination* (Basic books, 2008).
2. John, E. R. The neurophysics of consciousness. *Brain Res. Rev.* **39**, 1–28 (2002).
3. Llinás, R., Ribary, U., Contreras, D. & Pedroarena, C. The neuronal basis for consciousness. *Philosophical Trans. Royal Soc. Lond. Ser. B: Biol. Sci.* **353**, 1841–1849 (1998).
4. Jones, E. G. *The Thalamus* (Plenum, 1985).
5. Hwang, K., Bertolero, M. A., Liu, W. B. & D'Esposito, M. The human thalamus is an integrative hub for functional brain networks. *J. Neurosci.* **37**, 5594–5607 (2017).
6. Min, B. K., Kim, H. S., Pinotsis, D. A. & Pantazis, D. Thalamocortical inhibitory dynamics support conscious perception. *Neuroimage* **220**, 117066 (2020).
7. Seo, J., Kim, D. J., Choi, S. H., Kim, H. & Min, B. K. The thalamocortical inhibitory network controls human conscious perception. *NeuroImage* **264**, 119748 (2022).
8. Seo, J. & Min, B. K. Non-invasive electrical brain stimulation modulates human conscious perception of mental representation. *NeuroImage* **294**, 120647 (2024).
9. Min, B. K. A thalamic reticular networking model of consciousness. *Theor. Biol. Med. Model.* **7**, 10. https://doi.org/10.1186/1742-4682-7-10 (2010).
10. Sherman, S. M. Thalamus plays a central role in ongoing cortical functioning. *Nat. Neurosci.* **19**, 533–541. https://doi.org/10.1038/nn.4269 (2016).
11. Nekovarova, T., Fajnerova, I., Horacek, J. & Spaniel, F. Bridging disparate symptoms of schizophrenia: a triple network dysfunction theory. *Front. Behav. Neurosci.* **8**, 171 (2014).
12. Sridharan, D., Levitin, D. J. & Menon, V. A critical role for the right fronto-insular cortex in switching between central-executive and default-mode networks. *Proc. Natl. Acad. Sci.* **105**, 12569–12574 (2008).
13. Menon, V. & Uddin, L. Q. Saliency, switching, attention and control: a network model of insula function. *Brain Struct. function.* **214**, 655–667 (2010).
14. Peters, S. K., Dunlop, K. & Downar, J. Cortico-striatal-thalamic loop circuits of the salience network: a central pathway in psychiatric disease and treatment. *Front. Syst. Neurosci.* **10**, 104 (2016).
15. Seo, J., Lee, J. & Min, B. K. Out-of-phase transcranial alternating current stimulation modulates the neurodynamics of inhibitory control. *Neuroimage* **292**, 120612 (2024).
16. Kim, Y. et al. Neuromodulation of inhibitory control using phase-lagged transcranial alternating current stimulation. *J. Neuroeng. Rehabil.* **21**, 93 (2024).
17. Seo, J., Lee, D., Pantazis, D. & Min, B. K. Phase-lagged tACS between executive and default mode networks modulates working memory. *Sci. Rep.* **15** https://doi.org/10.1038/s41598-025-91881-5 (2025).
18. Menon, V. Large-scale brain networks and psychopathology: a unifying triple network model. *Trends Cogn. Sci.* **15**, 483–506 (2011).
19. Greicius, M. D., Krasnow, B., Reiss, A. L. & Menon, V. Functional connectivity in the resting brain: a network analysis of the default mode hypothesis. *Proc. Natl. Acad. Sci.* **100**, 253–258 (2003).
20. Fox, M. D., Corbetta, M., Snyder, A. Z., Vincent, J. L. & Raichle, M. E. Spontaneous neuronal activity distinguishes human dorsal and ventral attention systems. *Proc. Natl. Acad. Sci.* **103**, 10046–10051 (2006).
21. Raichle, M. E. et al. A default mode of brain function. *Proc. Natl. Acad. Sci.* **98**, 676–682 (2001).
22. Kong, R. et al. Individual-specific areal-level parcellations improve functional connectivity prediction of behavior. *Cereb. Cortex.* **31**, 4477–4500 (2021).
23. Rolls, E. T., Huang, C. C., Lin, C. P., Feng, J. & Joliot, M. Automated anatomical labelling atlas 3. *Neuroimage* **206**, 116189 (2020).
24. Setzer, B. et al. A temporal sequence of thalamic activity unfolds at transitions in behavioral arousal state. *Nat. Commun.* **13**, 5442 (2022).
25. Shine, J. M., Lewis, L. D., Garrett, D. D. & Hwang, K. The impact of the human thalamus on brain-wide information processing. *Nat. Rev. Neurosci.* **24**, 416–430 (2023).
26. McAlonan, K., Cavanaugh, J. & Wurtz, R. H. Guarding the gateway to cortex with attention in visual thalamus. *Nature* **456**, 391–394 (2008).
27. Corbetta, M. & Shulman, G. L. Control of goal-directed and stimulus-driven attention in the brain. *Nat. Rev. Neurosci.* **3**, 201–215 (2002).
28. Dosenbach, N. U., Fair, D. A., Cohen, A. L., Schlaggar, B. L. & Petersen, S. E. A dual-networks architecture of top-down control. *Trends Cogn. Sci.* **12**, 99–105 (2008).
29. Gent, T. C., Bandarabadi, M., Herrera, C. G. & Adamantidis, A. R. Thalamic dual control of sleep and wakefulness. *Nat. Neurosci.* **21**, 974–984 (2018).
30. Jang, S. H., Lim, H. W. & Yeo, S. S. The neural connectivity of the intralaminar thalamic nuclei in the human brain: a diffusion tensor tractography study. *Neurosci. Lett.* **579**, 140–144 (2014).
31. Pergola, G. et al. The regulatory role of the human mediodorsal thalamus. *Trends Cogn. Sci.* **22**, 1011–1025 (2018).
32. Mitchell, A. S. The mediodorsal thalamus as a higher order thalamic relay nucleus important for learning and decision-making. *Neurosci. Biobehavioral Reviews.* **54**, 76–88 (2015).
33. de Bourbon-Teles, J. et al. Thalamic control of human attention driven by memory and learning. *Curr. Biol.* **24**, 993–999 (2014).
34. Seeley, W. W. et al. Dissociable intrinsic connectivity networks for salience processing and executive control. *J. Neurosci.* **27**, 2349–2356 (2007).
35. Xiaob, D. & Barbas, H. Circuits through prefrontal cortex, basal ganglia, and ventral anterior nucleus map pathways beyond motor control. *Thalamus Relat. Syst.* **2**, 325–343 (2004).
36. Collins, D. P., Anastasiades, P. G., Marlin, J. J. & Carter, A. G. Reciprocal circuits linking the prefrontal cortex with dorsal and ventral thalamic nuclei. *Neuron* **98**, 366–379 (2018). e364.
37. Griffiths, B. J. et al. Rhythmic interactions between the mediodorsal thalamus and prefrontal cortex precede human visual perception. *Nat. Commun.* **13**, 3736 (2022).
38. Wolff, M. & Halassa, M. M. The mediodorsal thalamus in executive control. *Neuron* **112**, 893–908 (2024).
39. Parnaudeau, S., Bolkan, S. S. & Kellendonk, C. The mediodorsal thalamus: an essential partner of the prefrontal cortex for cognition. *Biol. Psychiatry.* **83**, 648–656 (2018).
40. Mengxing, L., Lerma-Usabiaga, G., Clascá, F. & Paz-Alonso, P. M. High-resolution tractography protocol to investigate the pathways between human mediodorsal thalamic nucleus and prefrontal cortex. *J. Neurosci.* **43**, 7780–7798 (2023).
41. Ouhaz, Z., Perry, B. A., Nakamura, K. & Mitchell, A. S. Mediodorsal thalamus is critical for updating during extradimensional shifts but not reversals in the attentional set-shifting task. *Eneuro* **9** (2022).
42. Watanabe, Y. & Funahashi, S. Thalamic mediodorsal nucleus and working memory. *Neurosci. Biobehavioral Reviews.* **36**, 134–142 (2012).
43. Mitchell, A. S. & Chakraborty, S. What does the mediodorsal thalamus do? *Front. Syst. Neurosci.* **7**, 37 (2013).
44. Fischer, J. & Whitney, D. Attention gates visual coding in the human pulvinar. *Nat. Commun.* **3**, 1051 (2012).
45. Basile, G. A. et al. The replication principle revisited: a shared functional organization between pulvinar-cortical and cortico-cortical connectivity and its structural and molecular imaging correlates. bioRxiv, 2024.2007. (2024). 2011.603063.
46. Zhou, H., Schafer, R. J. & Desimone, R. Pulvinar-cortex interactions in vision and attention. *Neuron* **89**, 209–220 (2016).

47. Njemanze, P. C., Gomez, C. R. & Horenstein, S. Cerebral lateralization and color perception: a transcranial Doppler study. *Cortex* **28**, 69–75 (1992).
48. Rubino, C. Hemispheric lateralization of visual perception. *Cortex* **6**, 102–120 (1970).
49. Gotts, S. J. et al. Two distinct forms of functional lateralization in the human brain. *Proc. Natl. Acad. Sci.* **110**, E3435–E3444 (2013).
50. Allison, T., McCarthy, G., Nobre, A., Puce, A. & Belger, A. Human extrastriate visual cortex and the perception of faces, words, numbers, and colors. *Cereb. Cortex*. **4**, 544–554 (1994).
51. Spiridon, M., Fischl, B. & Kanwisher, N. Location and spatial profile of category-specific regions in human extrastriate cortex. *Hum. Brain. Mapp.* **27**, 77–89 (2006).
52. Sakai, K. et al. Functional mapping of the human colour centre with echo-planar magnetic resonance imaging. *Proc. R. Soc. Lond. B Biol. Sci.* **261**, 89–98 (1995).
53. Wang, X. et al. Where color rests: spontaneous brain activity of bilateral fusiform and lingual regions predicts object color knowledge performance. *Neuroimage* **76**, 252–263 (2013).
54. Wallis, J. D. Orbitofrontal cortex and its contribution to decision-making. *Annu. Rev. Neurosci.* **30**, 31–56 (2007).
55. Klein-Flügge, M. C., Bongioanni, A. & Rushworth, M. F. Medial and orbital frontal cortex in decision-making and flexible behavior. *Neuron* **110**, 2743–2770 (2022).
56. Chang, C. & Grace, A. A. Inhibitory modulation of orbitofrontal cortex on medial prefrontal cortex–amygdala information flow. *Cereb. Cortex*. **28**, 1–8 (2018).
57. Rizzolatti, G., Ferrari, P. F., Rozzi, S. & Fogassi, L. In *Percept, Decision, Action: Bridging the Gaps: Novartis Foundation Symposium* 270. 129–145 (Wiley Online Library).
58. Rubia, K., Smith, A. B., Brammer, M. J. & Taylor, E. Right inferior prefrontal cortex mediates response inhibition while mesial prefrontal cortex is responsible for error detection. *Neuroimage* **20**, 351–358 (2003).
59. Baldo, J. V. & Dronkers, N. F. The role of inferior parietal and inferior frontal cortex in working memory. *Neuropsychology* **20**, 529 (2006).
60. Bowmaker, J. K. & Dartnall, H. Visual pigments of rods and cones in a human retina. *J. Physiol.* **298**, 501–511 (1980).
61. Di Lollo, V., Clark, C. D. & Hogben, J. H. Separating visible persistence from retinal afterimages. *Percept. Psychophys.* **44**, 363–368 (1988).
62. Thielscher, A., Antunes, A. & Saturnino, G. B. In *2015 37th annual international conference of the IEEE engineering in medicine and biology society (EMBC)*. 222–225 (IEEE).
63. Brincat, S. L. & Miller, E. K. Prefrontal cortex networks shift from external to internal modes during learning. *J. Neurosci.* **36**, 9739–9754 (2016).
64. Miller, E. K., Lundqvist, M. & Bastos, A. M. *Working Memory 2 0 Neuron* **100**, 463–475 (2018).
65. Min, B. K. et al. Electrophysiological decoding of spatial and color processing in human prefrontal cortex. *NeuroImage* **237**, 118165 (2021).
66. Power, J. D., Barnes, K. A., Snyder, A. Z., Schlaggar, B. L. & Petersen, S. E. Spurious but systematic correlations in functional connectivity MRI networks arise from subject motion. *Neuroimage* **59**, 2142–2154 (2012).
67. Taylor, J., Rastle, K. & Davis, M. H. Interpreting response time effects in functional imaging studies. *Neuroimage* **99**, 419–433 (2014).
68. Thomas, J. B. et al. Functional connectivity in autosomal dominant and late-onset Alzheimer disease. *JAMA Neurol.* **71**, 1111–1122 (2014).
69. Weissenbacher, A. et al. Correlations and anticorrelations in resting-state functional connectivity MRI: a quantitative comparison of preprocessing strategies. *Neuroimage* **47**, 1408–1416 (2009).
70. Yuen, N. H., Osachoff, N. & Chen, J. J. Intrinsic frequencies of the resting-state fMRI signal: the frequency dependence of functional connectivity and the effect of mode mixing. *Front. NeuroSci.* **13**, 900 (2019).
71. Rubinov, M. & Sporns, O. Weight-conserving characterization of complex functional brain networks. *Neuroimage* **56**, 2068–2079 (2011).
72. Cheng, H. & Liu, J. Concurrent brain parcellation and connectivity estimation via co-clustering of resting state fMRI data: A novel approach. *Hum. Brain. Mapp.* **42**, 2477–2489 (2021).
73. Lancichinetti, A. & Fortunato, S. Consensus clustering in complex networks. *Sci. Rep.* **2**, 336 (2012).
74. Newman, M. E. Modularity and community structure in networks. *Proc. Natl. Acad. Sci.* **103**, 8577–8582 (2006).
75. Clauset, A., Newman, M. E. & Moore, C. Finding community structure in very large networks. *Phys. Rev. E—Statistical Nonlinear Soft Matter Phys.* **70**, 066111 (2004).
76. Rubinov, M., Kötter, R., Hagmann, P. & Sporns, O. Brain connectivity toolbox: a collection of complex network measurements and brain connectivity datasets. *NeuroImage* **47**, S169 (2009).
77. Rubinov, M. & Sporns, O. Complex network measures of brain connectivity: uses and interpretations. *Neuroimage* **52**, 1059–1069 (2010).

Acknowledgements

We thank Je-Choon Park, Jeongwook Kwon, Yukyung Kim, Sangbin Yun, and Jaewon Yang for their assistance with fMRI data acquisition and tACS administration. We also thank Dr. Dongha Lee for his kind work in drawing Fig. 1.

Author contributions

Seulgi Lee: Investigation, Formal analysis, Methodology, Visualization, Writing - Original draft. Bumhee Park: Investigation, Software, Formal analysis, Methodology, Visualization, Writing - Original draft, Funding acquisition. Jeehye Seo: Investigation, Formal analysis. Byoung-Kyong Min: Conceptualization, Methodology, Investigation, Formal analysis, Writing - Original draft, Reviewing and Editing, Supervision, Project administration, Funding acquisition.

Funding

This work was supported by the New Faculty Startup Fund from Seoul National University and the National Research Foundation of Korea (NRF) grant funded by the Korea government (MSIT) (grant number RS-2025-00513128 to B.-K.M. and NRF-2019R1A5A2026045 to B.P.).

Declarations

Competing interests

The authors declare no competing interests.

Ethics approval

The study complied with ethical guidelines established by the Institutional Review Board of Korea University (Approval No. KUIRB-2021–0209–08) and the Declaration of Helsinki (World Medical Association, 2013).

Consent to participate

Informed consent was obtained from all individual participants included in the study.

Additional information

Supplementary Information The online version contains supplementary material available at https://doi.org/10.1038/s41598-026-48061-w.

Correspondence and requests for materials should be addressed to B.-K.M.

Reprints and permissions information is available at www.nature.com/reprints.

Publisher's note Springer Nature remains neutral with regard to jurisdictional claims in published maps and institutional affiliations.